Available online at www.sciencedirect.com
ScienceDirect
Tetrahedron 64 (2008) 1839–1846
Tetrahedron
www.elsevier.com/locate/tet

Programmable conformational regulation of porphyrin dimers on geometric scaffold of duplex DNA

Masayuki Endo*, Mamoru Fujitsuka, Tetsuro Majima*

The Institute of Scientific and Industrial Research, Osaka University, 8-1 Mihogaoka, Ibaraki, Osaka 567-0047, Japan

Received 4 October 2007; received in revised form 28 November 2007; accepted 28 November 2007
Available online 4 December 2007

This paper is dedicated to Professor Isao Saito on the occasion of his 65th birthday

Abstract

DNA–porphyrin conjugates were designed and synthesized in which free-base and Zn-coordinated porphyrins were introduced to the N^6-position of the internal adenosine. Conformations of the porphyrin dimer in the major groove of duplex DNA were controlled by changing the orientation and the distance between the two porphyrin moieties. The porphyrin dimers formed a thermally favorable face-to-face conformation on the duplex DNA. In the disadvantageous geometry for porphyrin dimer formation on the duplex, the porphyrins induced the DNA duplex structures to the *Z*-form conformation. These results indicate that the interaction of the two porphyrins and the conformation of duplex DNA are controlled by the program of DNA sequences.

1. Introduction

Suitable arrangement of multiple chromophores is one of the most crucial issues in the materials science, since the self-assembled multi-chromophore system finally shows the completely different physical, photochemical, electrochemical properties.[1–5] Porphyrin derivatives have been widely investigated because of their characteristic H- and J-aggregates formation under specific conditions and their useful photophysical and electrochemical properties.[6–10] For the construction of structurally controlled arrays of functional molecules, DNA can provide a useful scaffold for attachment and arrangement of the desired molecules. Recently, multiple pyrenes have been introduced onto the DNA and RNA, which form structurally defined pyrene arrays and display different photophysical properties from the monomer as investigated by a spectroscopic analysis.[11,12]

In this study, we intended to prepare structurally controlled porphyrin dimers on the duplex DNA. We introduced free-base porphyrin (FbP) and Zn-coordinated porphyrin (ZnP) into the N^6-position of adenine base via a linker (Fig. 1A). Two porphyrins were introduced to the duplex DNA using the self-complementary sequences. We designed the DNA–porphyrin conjugates based on the following four points: (i) negative charges were introduced to the porphyrin derivatives to prevent the undesired interaction with duplex DNA; (ii) two porphyrins which were introduced to adjacent base pairs (**1** and **2**) and those separated by two base pairs (**3** and **4**); (iii) the two N^6-amino groups of adenosine were located in close (**1** and **3**) and far (**2** and **4**) sites on the duplex DNA; (iv) the tethers attached to the porphyrins oriented to the similar directions (AT/AT sequence; **1** and **3**) and the different ones (TA/TA sequence; **2** and **4**) during base pairing (Fig. 1B).[13] Because of the right-handed helical geometry of duplex DNA, these differences should appear and affect the porphyrin dimer formation. Using this design, we investigated the interaction of the porphyrin derivatives on the duplex DNA scaffolds.

2. Results and discussion

2.1. Preparation of DNA–porphyrin conjugates

Tetraphenylporphyrin derivatives **5** (FbP) and **6** (ZnP) were synthesized, which have three sulfonate groups for

* Corresponding authors. Tel.: +81 6 6879 8495; fax: +81 6 6879 8499.
E-mail addresses: endo@sanken.osaka-u.ac.jp (M. Endo), majima@sanken.osaka-u.ac.jp (T. Majima).

0040-4020/$ - see front matter © 2007 Published by Elsevier Ltd.
doi:10.1016/j.tet.2007.11.096

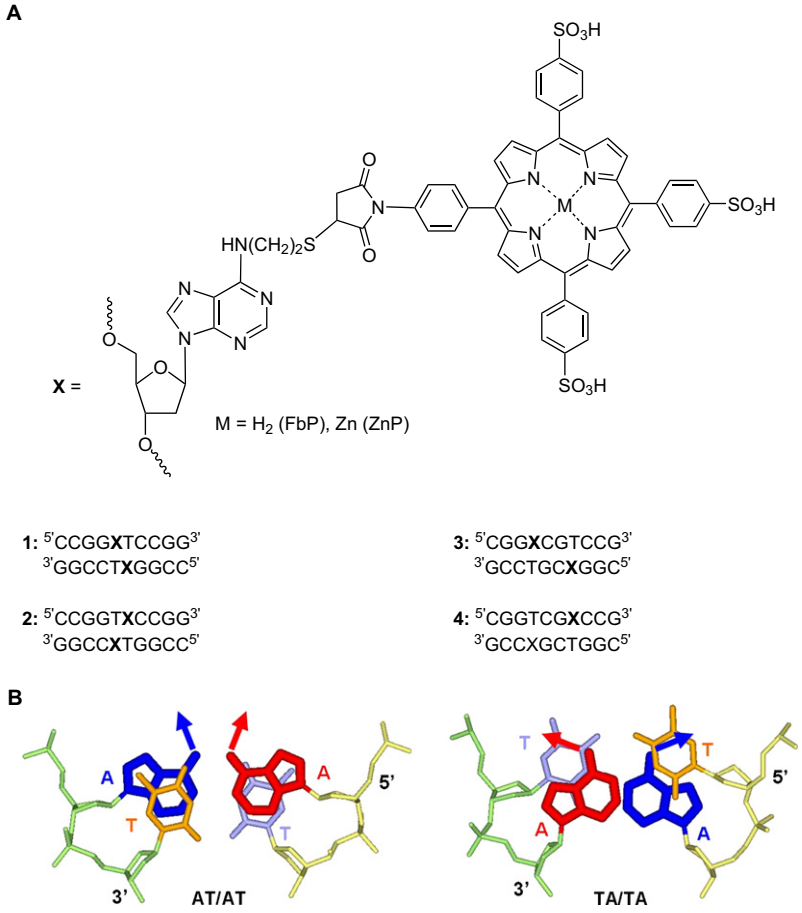

Figure 1. DNA–porphyrin conjugates used in the experiments. (A) Structure of DNA–free-base porphyrin (FbP) and Zn-coordinated porphyrin (ZnP) conjugates, where tri(sulfonatophenyl)succinimidophenyl-porphyrin is introduced to the N^6-position of deoxyadenosine via ethylthiol linker. Four DNA sequences containing porphyrin derivatives (denoted as X). (B) Base pairing geometry of AT/AT and TA/TA sequences. Arrows represent the direction of the tethers.[15]

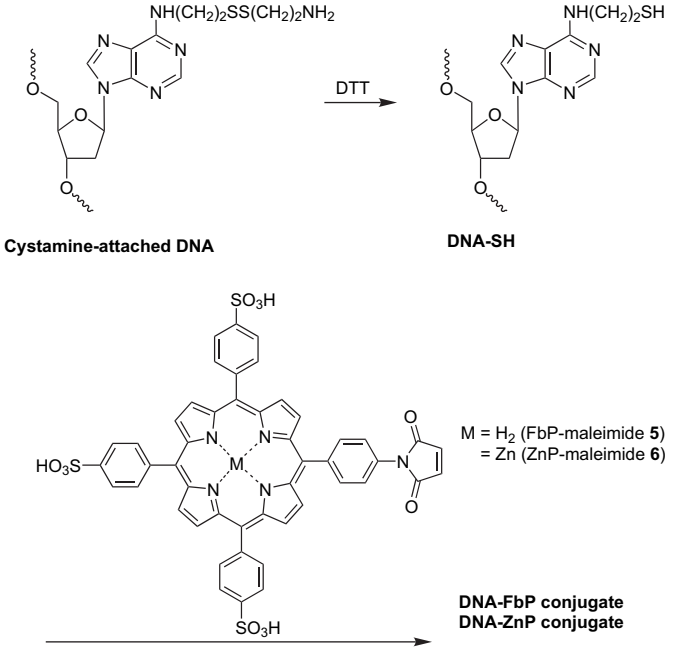

Scheme 1. Synthesis of DNA–porphyrin conjugates.

water-solubility and a maleimide group for coupling with thiol group (Scheme 1). Introduction of maleimide group to 5-(4-aminophenyl)-10,15,20-tri(4-sulfonatophenyl)porphyrin[14] was carried out using maleic anhydride, followed by treatment with sodium bicarbonate and acetic anhydride. Zinc was introduced to the porphyrin using zinc acetate with heating. Introduction of porphyrin derivatives into the N^6-position of an internal 2′-deoxyadenosine[13] was carried out using the coupling reaction of porphyrin maleimide with thiol linker attached to the N^6-position of adenosine in the oligonucleotides (Scheme 1). Cystamine-attached DNA was reduced with DTT, and then porphyrin derivatives were coupled to DNA containing N^6-mercaptoethyl-2′-deoxyadenosine using FbP-maleimide **5** or ZnP-maleimide **6**. The production of DNA–porphyrin conjugates was confirmed by MALDI-TOF MS spectroscopy.

2.2. Temperature-dependent UV–vis spectral change of porphyrin region during duplex formation

To investigate the interaction of the two porphyrins, UV–vis spectra were measured by changing the temperature of the samples. The spectral change in the Soret band of the porphyrin moieties depending on the temperature was

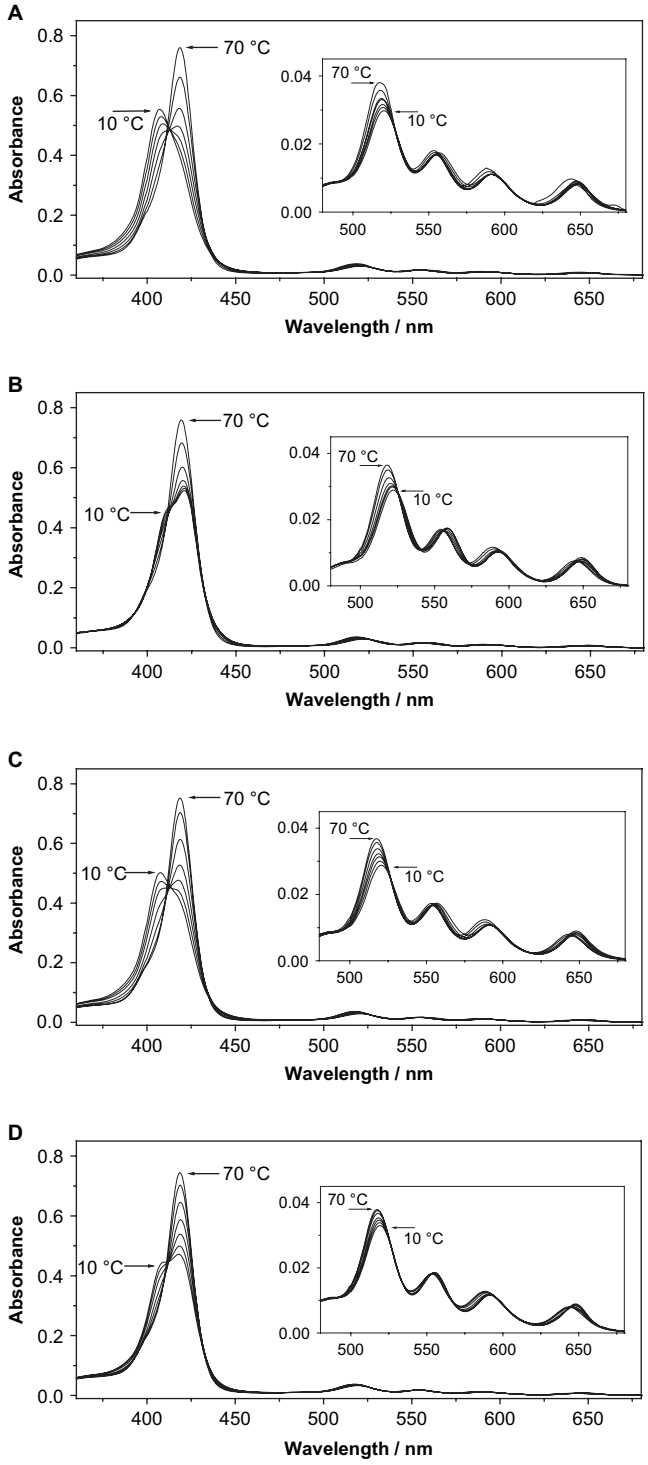

Figure 2. Temperature-dependent UV–vis spectra of DNA–free-base porphyirn conjugates. (A) **1-FbP**; (B) **2-FbP**; (C) **3-FbP**; (D) **4-FbP**. Temperature was increased every 10 °C from 10 °C to 70 °C. Insets represent the Q-band region.

investigated (Fig. 2). In the case of the **1-FbP** (Fig. 2A), a clear peak split of the Soret bands (407 nm at 10 °C and 418 nm at 70 °C) was observed by changing the temperature. By decreasing the temperature, the peaks gradually shifted to a shorter wavelength with decreasing absorbance of the peaks. The absorbance of the peaks significantly changed below 40 °C, which corresponds to the association of the DNA strands. By comparing the dissociated state of DNA at 70 °C with duplex state at 10 °C, the peaks shifted to a shorter wavelength by 11 nm accompanied by broadening of the peaks, which is assigned to the face-to-face overlap of two porphyrins (or H-aggregate).[6–8] During the duplex formation at lower temperature (10–30 °C), the Soret band of the porphyrin shifted to 407 nm with increasing absorbance, indicating the conformational change of porphyrin dimer. In contrast, the **2-FbP** (Fig. 2B) formed clearly different porphyrin dimer. Although the spectral change and peak shift of the Soret bands were observed by changing the temperature, the peak shifted to a longer wavelength from 418 nm at 70 °C to 421 nm at 10 °C. At lower temperature (10–30 °C), the porphyrin dimer formed a complex with slight change in the spectra. As compared to the spectrum of porphyrin dimer in the **1-FbP** duplex with that in the **2-FbP** duplex at 10 °C, the obvious difference is attributed to the sequences and orientations of the tethers attaching FbP to N^6-position of adenine base. As shown in Figure 1B, the alkyl chains attached to the N^6-position of adenine in the **1-FbP** duplex oriented to the similar direction in the major groove for the favorable face-to-face overlap of the porphyrin dimer. On the other hand, the alkyl chains in the **2-FbP** duplex oriented to the outer direction, which causes disadvantage for the favorable FbP dimer overlap. These indicate that the double helix DNA scaffold structurally controls the conformation of the FbP dimer.

In the cases of the **3-FbP** and **4-FbP** duplex having two porphyrins separated by two base pairs, the FbP dimer in the **3-FbP** duplex showed an almost similar spectral change as compared to that in the **1-FbP** duplex. The FbP dimer in the **4-FbP** duplex showed a weaker H-aggregate band as compared to that in the **3-FbP** duplex. Because the porphyrins were separated by two base pairs and contacted loosely, the spectral difference between the **3-FbP** and **4-FbP** was observed as modest way as compared to that between the **1-FbP** and **2-FbP**.

We also examined the temperature-dependent spectral changes of the DNA–ZnP conjugates (Fig. 3). As similar to the spectra of the DNA–FbP conjugates, **1-ZnP** and **3-ZnP** showed a short wavelength shift and decrease in absorbance at lower temperature. On the other hand, the spectral changes of **2-ZnP** and **4-ZnP** were modest, suggesting that the weak interaction between the two ZnPs may be attributed to the destabilization of the interaction by coordination of Zn ion to the porphyrin moiety. Because the zinc is located out of the porphyrin plane and a water molecule occupies an axial position of zinc, coordination of zinc prevents the interaction of porphyrins as compared to that of FbP.[18,19] From the melting temperature, zinc ion coordination destabilizes the interaction of porphyrins as well as the duplex formation.

2.3. Porphyrin interaction on duplex DNA investigated by CD spectroscopy

The interaction of the porphyrin moieties and DNA backbone structures were examined by circular dichroism (CD)

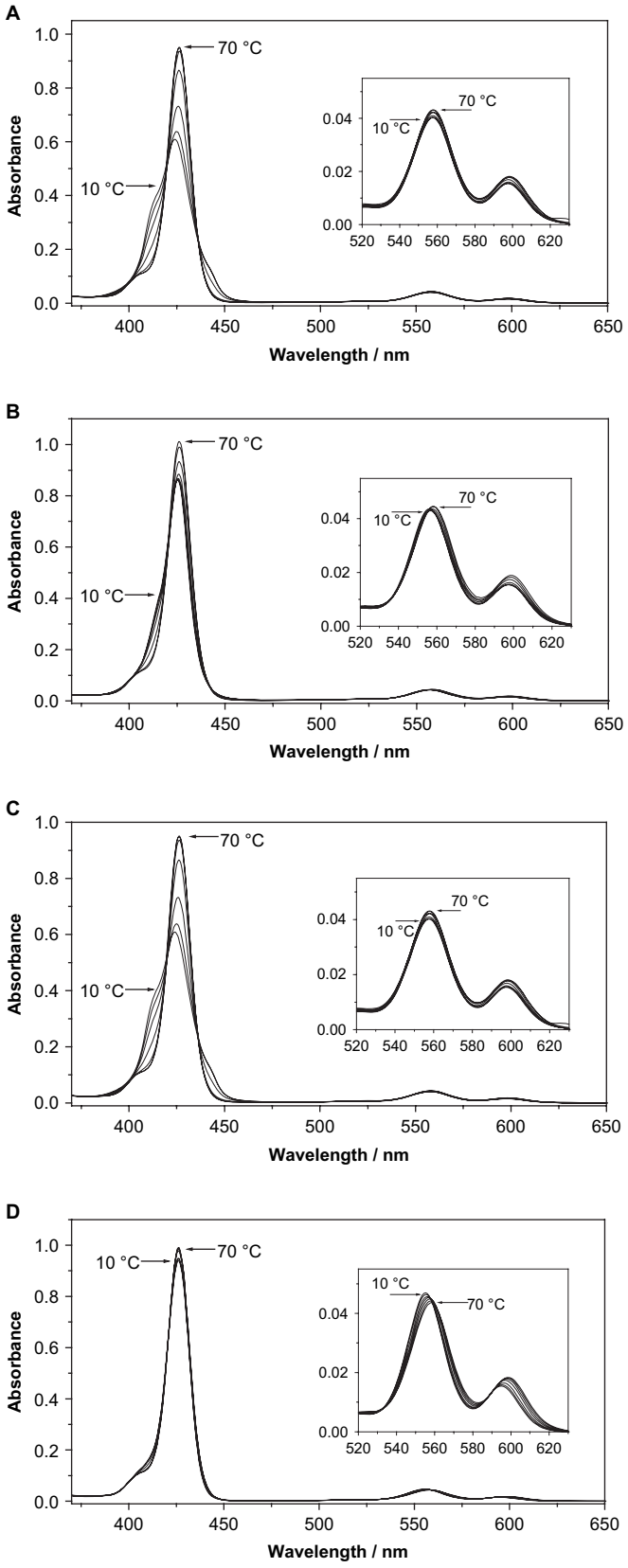

Figure 3. Temperature-dependent UV–vis spectra of DNA–Zn-porphyirn conjugates. (A) **1-ZnP**; (B) **2-ZnP**; (C) **3-ZnP**; (D) **4-ZnP**. Temperature was increased every 10 °C from 10 °C to 70 °C. Insets represent the Q-band region.

spectroscopy (Fig. 4). We investigated both the characteristic CD bands of duplex DNA and porphyrin moieties. In the CD spectra of all the DNA–porphyrin conjugates, induced CD bands originating from the Soret band of the porphyrin derivatives were observed around 400–450 nm. The **1-FbP** and **2-FbP** showed different induced CD bands in the porphyrin regions (Fig. 4A). In the case of the **1-FbP**, strong negative and positive bands appeared around 415 nm and 440 nm, respectively. In contrast, positive and weaker negative bands were observed in the **2-FbP** at 408 nm and 424 nm, respectively. Appearance of positive and negative CD bands indicates the excitonic coupling between two porphyrin chromophores.[16–18] The differences in the CD bands of the porphyrin region between the **1-FbP** and **2-FbP** are attributed to the difference in the overlap of the two transition dipoles of porphyrins.[20] In the case of the **1-FbP**, the observed positive CD exciton couplet in the spectrum indicates the clockwise overlap of the transition dipoles. In contrast, the spectrum in the **2-FbP** showed the negative CD exciton couplet, which indicates the counterclockwise overlap of the transition dipoles. The backbones of the DNA structures were also characterized. In the DNA structure of the **1-FbP**, the negative and positive bands (240 nm and 265 nm, respectively) were observed, which are characteristic for a *B*-form double helix structure.[21] In contrast, the different CD bands, negative (240 nm and 280 nm) and positive (260 nm) bands appeared, in the **2-FbP**, suggesting the formation of *Z*-form duplex.[21] The TA/TA step is easily unwound because of the smaller overlap of the adjacent base pairs as compared to that in the AT/AT step (Fig. 1B).[22] This may also help the formation of *Z*-form in the **2-FbP** duplex.

For the **3-FbP** and **4-FbP** (Fig. 4B), both DNAs formed *B*-form duplex structures. The **3-FbP** and **4-FbP** showed different induced CD bands in the porphyrin regions. In the case of the **3-FbP**, strong negative and positive bands appeared around 415 nm and 437 nm, respectively. In contrast, weaker positive and negative bands were observed in the **4-FbP** around 420 nm and 450 nm, respectively. The different CD bands in the porphyrin region originated from the different direction of the two transition dipoles of porphyrins in the **3-FbP** and **4-FbP**. In spite of the two porphyrins being separated by two base pairs, the CD band in the Soret-band region of the **3-FbP** showed a similar intensity as compared to that of the **1-FbP**, indicating the flexible contact of the two porphyrins. Excition couplet of the **4-FbP** was very weak because of the disadvantageous geometry on the duplex DNA.

We also examined the DNA structures and porphyrin interaction of the ZnP-attached DNAs by CD spectroscopy. In the cases of **1-ZnP** and **2-ZnP**, quite strong CD bands in the porphyrin region were observed. The **1-ZnP** and **2-ZnP** showed different induced CD bands in the porphyrin regions (Fig. 4C). For the **1-ZnP**, strong negative and positive bands appeared at 420 nm and 432 nm, respectively. In contrast, positive and negative bands were observed in the **2-ZnP** at 419 nm and 428 nm, respectively. The differences in the CD bands of porphyrin region between the **1-ZnP** and **2-ZnP** are also attributed to the difference in the overlap of the

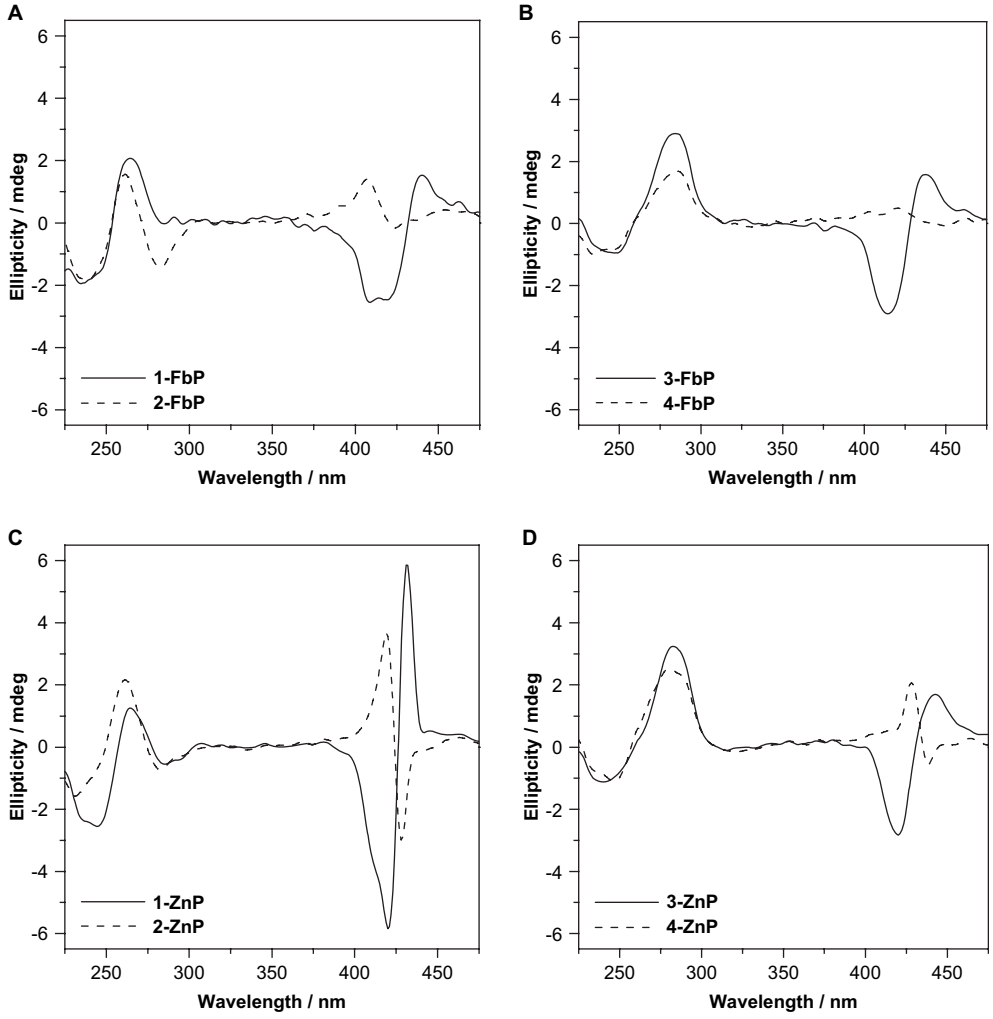

Figure 4. CD spectra of the DNA–porphyrin conjugates. (A) **1-FbP** (solid line) and **2-FbP** (broken line); (B) **3-FbP** (solid line) and **4-FbP** (broken line); (C) **1-ZnP** (solid line) and **2-ZnP** (broken line); (D) **3-ZnP** (solid line) and **4-ZnP** (broken line).

transition dipoles of the two ZnPs as similar to the **1-FbP** and **2-FbP**. In the backbones of the duplexes, both DNAs showed partial *Z*-form duplex structures, meaning that the ZnP dimer induces duplex to the *Z*-form structure. Direct overlap of the ZnPs may not be structurally favorable because of the location of Zn in the porphyrin and coordination of water onto Zn,[18,19] which may induce a different duplex conformation of the **1-ZnP** as compared to that of the **1-FbP** duplex.

For the **3-ZnP** and **4-ZnP** (Fig. 4D), both formed *B*-form duplex structures. The **3-ZnP** and **4-ZnP** also showed different induced CD bands in the porphyrin regions. In the case of the **3-ZnP**, strong negative and positive bands appeared around 420 nm and 442 nm, respectively. In contrast, positive and negative bands were observed in the **3-FbP** at 427 nm and 438 nm, respectively.

These results suggest that the two orientations of the porphyrin dimers can be characterized by induced CD bands in the porphyrin regions, whose differences reflect the different overlap of the two porphyrins. Some porphyin–porphyrin interactions induce the *Z*-form duplex formation, because of the strong interaction of two adjacent porphyrins.

2.4. Fluorescence properties of porphyrins on the duplex DNA

Fluorescence spectra of the DNA–porphyrin conjugates in the DNA were investigated (Fig. 5). For the DNA–FbP, we used the two wavelengths for excitation: one is the peak top (407 nm) at 10 °C in the UV–vis spectra where porphyrins form aggregated structures and the other is that (418 nm) at 70 °C where porphyrins are monomeric. The data are summarized in Table 1. From all the DNA–FbP conjugates, the emission peaks excited at 418 nm shifted to a longer wavelength than the corresponding peaks excited at 407 nm. Emission peaks of the **2-FbP** and **4-FbP** showed the shorter wavelengths up to 6 nm as compared to those of the **1-FbP** and **3-FbP**, respectively. Fluorescence lifetimes of FbP in the DNA–FbP conjugates were also measured (Table 1). Fluorescence lifetimes of the **1-FbP** and **3-FbP** showed two components with relatively short values as compared to that of the monomeric porphyrin, meaning that these form similar porphyrin dimer conformation. On the other hand, the **2-FbP** and **4-FbP** showed single lifetime component. For the **2-FbP**, the lifetime is longer than those of

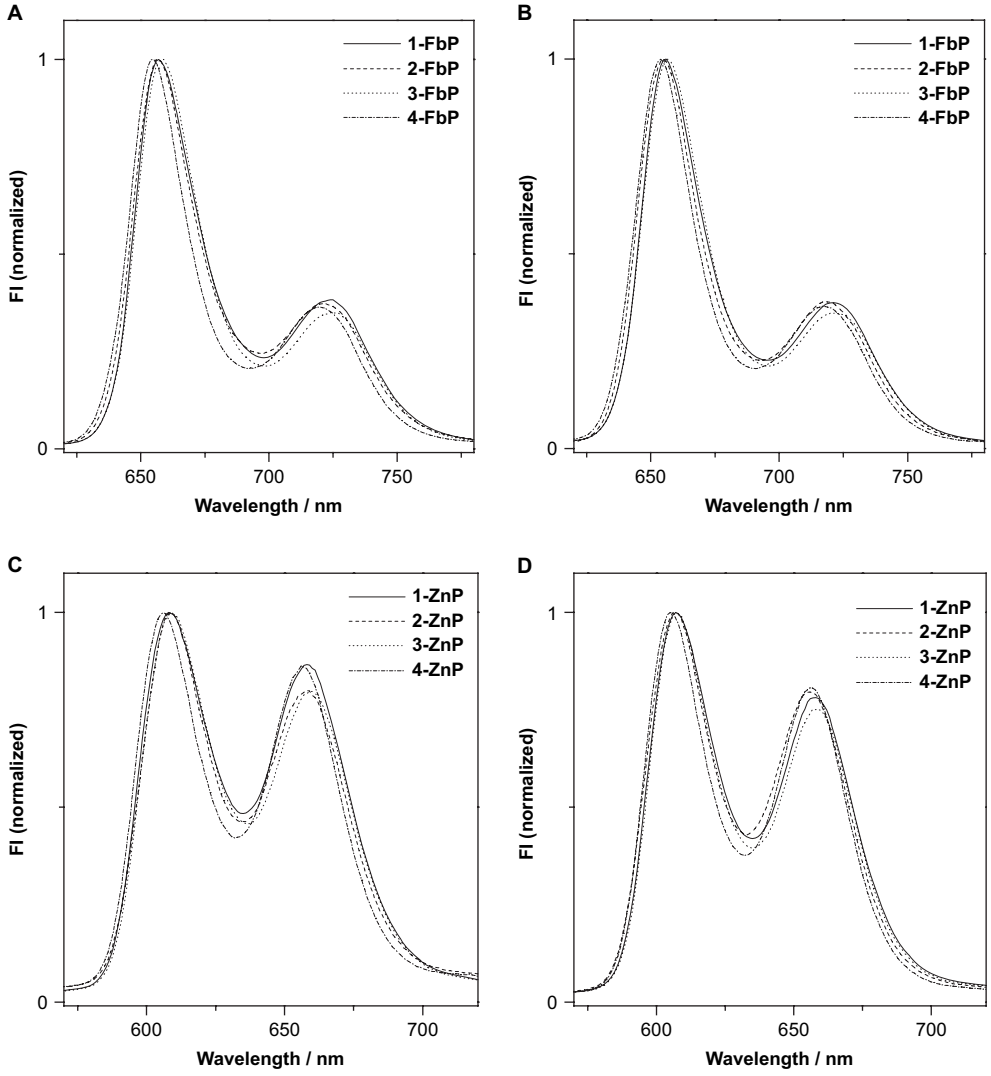

Figure 5. Fluorescence spectra of the DNA–porphyrin conjugates. (A) Emission spectra of DNA–FbP conjugates excited at 407 nm. (B) Emission spectra of DNA–FbP conjugates excited at 418 nm. (C) Emission spectra of DNA–ZnP conjugates excited at 412 nm. (D) Emission spectra of DNA–ZnP conjugates excited at 426 nm.

Table 1
Fluorescence properties of DNA–FbP conjugates[a]

DNA	Emission peaks/nm		τ_f/ns
	λ_{ex}=407 nm	λ_{ex}=418 nm	
1-FbP	657, 724	655, 721	2.63 (51%), 5.95 (49%)
2-FbP	657, 721	655, 718	11.26 (100%)
3-FbP	658, 725	657, 722	2.66 (53%), 6.04 (47%)
4-FbP	654, 719	653, 717	7.01 (100%)

[a] Measurement conditions are described in the experimental section. τ_f represents fluorescence lifetime.

Table 2
Fluorescence properties of DNA–ZnP conjugates[a]

DNA	Emission peaks/nm		τ_f/ns
	λ_{ex}=412 nm	λ_{ex}=426 nm	
1-ZnP	608, 658	607, 658	2.13
2-ZnP	609, 658	607, 656	2.09
3-ZnP	609, 659	607, 658	2.13
4-ZnP	606, 656	605, 656	2.27

[a] Measurement conditions are described in the experimental section. τ_f represents fluorescence lifetime.

the other DNA–FbP conjugates, suggesting that the poor overlap of the two porphyrins would occur in the **2-FbP**.

The fluorescence properties of the DNA–ZnP conjugates are summarized in Table 2. Two wavelengths for excitation were used for the DNA–ZnP conjugates: one is the shoulder of 412 nm (10 °C) originated from the aggregation in the UV–vis spectra and the other is a monomeric peak of 426 nm (70 °C). Similar to the spectra of the DNA–FbP conjugates, the emission peaks excited at 426 nm shifted to a longer wavelength than the corresponding peaks excited at 412 nm. The **1-ZnP** and **3-ZnP** showed the same tendency. In contrast, the **2-ZnP** and **4-ZnP** showed specific fluorescence properties, however, the differences are not so clear as compared to the corresponding DNA–FbP conjugates.

Molecular modeling of the porphyrin dimer on the DNA–FbP conjugates shows that the two porphyrins in the **1-FbP**

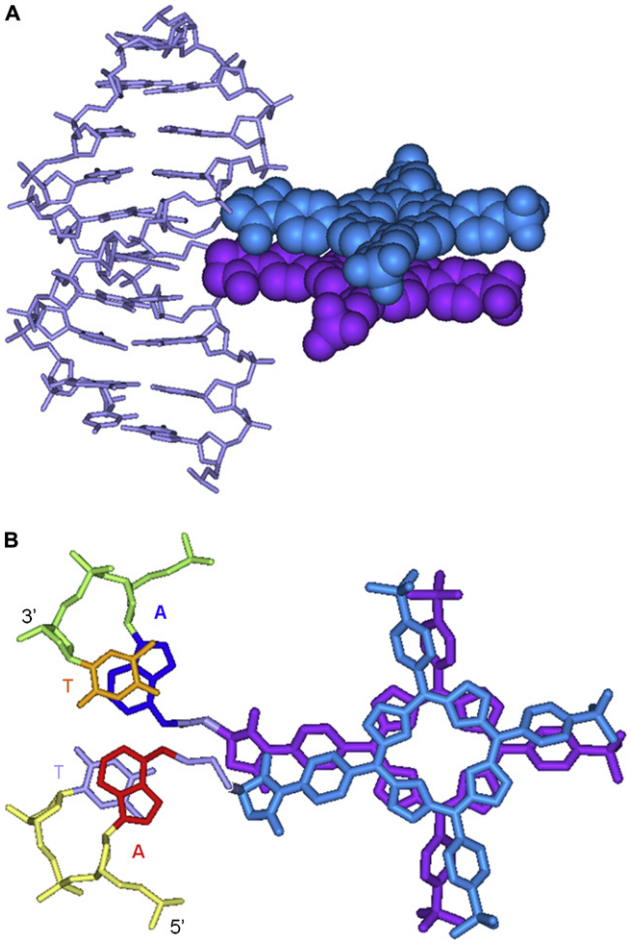

Figure 6. Model of porphyrin dimer conformation on the duplex. (A) Porphyrin dimer in the **1-FbP**. (B) Porphyrin conformation in AT/AT sequence, referring to the positive CD exciton couplet.

duplex form a cofacial conformation where the FbPs overlap clockwise (Fig. 6). The two porphyrins in the **2-FbP** duplex may form a conformation with different orientation of the transition dipoles from that of the **1-FbP**. The differences in the absorbance and CD spectra between the **1-FbP** and **2-FbP** reflect the different conformations and overlaps of the transition dipoles of the porphyrin dimers, which are induced by the geometry of the duplex structures.

3. Conclusions

We have designed and synthesized DNA–porphyrin conjugates, in which porphyrin derivatives including free-base and Zn-coordinated porphyrins have been introduced to the N^6-position of an internal adenosine. In the self-assembly process of DNA and porphyrin derivatives, the duplex formation occurs first by decreasing the temperature, and then the two porphyrins approach to form a dimer structure. By further decreasing the temperature, the porphyrin dimer changes the conformation on the duplex DNA to form the thermally favorable face-to-face overlapped conformation. In contrast, in the disadvantageous geometry for porphyrin dimer formation on the duplex, the porphyrins induced a conformational change of duplex to the *Z*-form structures. These indicate that the interaction of two porphyrin moieties and conformation of duplex DNA are controlled by the programs of DNA sequences. Using the selective assembly of the duplex DNA, the heterogeneous porphyrins and other chromophores can be introduced into the major groove of the DNA. These DNA–chromophore conjugates can be expanded for the construction of DNA-assisted and structurally controlled multi-chromophore arrays.

4. Experimental

4.1. General

All the reagents for DNA synthesis were obtained from Glen Research (Sterling, VA). DNA synthesis was performed on ABI 3800 DNA synthesizer. Purification of oligonucleotides was carried out on a JASCO LC-2000Plus series HPLC system. MALDI-TOF mass spectra were obtained on a Shimadzu AXIMA spectrometer. UV–vis and fluorescence spectra were obtained on a JASCO V-530 spectrophotometer and Hitachi F-850 spectrofluorometer, respectively.

4.2. Synthesis of porphyrin derivatives

4.2.1. 5-(4-Maleimidophenyl)-10,15,20-tri(4-sulfonatophenyl)porphyrin, tris(n-tetrabutylammonium) salt (*5*)

Maleic anhydride (3.0 mg, 0.030 mmol) was added to 5-(4-aminophenyl)-10,15,20-tri(4-sulfonatophenyl)porphyrin, tris-(tetrabutylammonium) salt (33 mg, 0.020 mmol)[13] dissolved in 2 mL dry CH_3CN and then the mixture was refluxed for 5 h. After the removal of solvent under reduced pressure, the reaction mixture was dissolved in 2 mL of acetic anhydride, and sodium bicarbonate (2.4 mg, 0.030 mmol) was added to the mixture. The reaction mixture was stirred at 80 °C for 1.5 h. After the removal of the solvent under reduced pressure, the mixture was dissolved in 50 mL of chloroform, and the organic layer was washed with 50 mL of water three times. After the chloroform layer was dried over sodium sulfate, the solvent was removed under reduced pressure, 30 mg (90% yield). ^{1}H NMR [$CDCl_3$/CD_3OD=5/1(TMS)] δ 8.93 (br s, 4H), 8.82 (br s, 4H), 8.31 (m, 8H), 8.22 (d, J=8.1 Hz, 6H), 7.78 (d, J=8.4 Hz, 2H), 7.02 (s, 2H), 3.30 (m, 24H), 1.68 (m, 24H), 1.45 (m, 24H), 1.04 (t, J=7.6 Hz, 36H). MALDI-TOF MS (positive) calcd 950.1 $[M+H]^+$, found 950.3.

4.2.2. 5-(4-Maleimidophenyl)-10,15,20-tri(4-sulfonatophenyl)zinc porphyrin, tris(n-tetrabutylammonium) salt (*6*)

Aqueous zinc acetate (10 mM, 0.4 mL) was added to **5** (10 mg, 6 mmol) dissolved in 50 μL of CH_3CN, and then the mixture was heated at 50 °C for 4 h. The product was extracted three times with chloroform (0.5 mL), and the organic layer was washed with 0.5 mL of water three times. The chloroform layer was dried under reduced pressure, 10 mg (95% yield). ^{1}H NMR [$CDCl_3$/CD_3OD=5/1(TMS)] δ 8.88 (m, 4H), 8.82 (s, 4H), 8.26 (m, 14H), 7.75 (d, J=8.4 Hz, 2H), 7.05 (s, 2H), 3.24 (m, 24H), 1.68 (m, 24H), 1.45 (m, 24H),

1.03 (t, J=7.3 Hz, 36H). MALDI-TOF MS (positive) calcd 1012.0 $[M+H]^+$, found 1013.0.

4.3. Synthesis of DNA–porphyrin conjugates

Cystamine was introduced to the N^6-position of adenine base by aminolysis of O^6-phenyl-2′-deoxyinosine in the synthetic oligonucleotides.[13] Purified cystamine-attached oligonucleotides (20 nmol) were treated with 1 mM DTT in 50 mM tris buffer (pH 8) at 50 °C for 30 min, and then purified on a reversed-phase HPLC (2–50% gradient of the same elution buffer). Porphyrin derivatives were coupled to N^6-mercaptoethyl-2′-deoxyadenosine-containing oligomers using 2 μL of 50 mM 5-(4-aminophenyl)-10,15,20-tri(4-maleimidophenyl)-porphyrin, tris(tetrabutylammonium) salt (FbP-maleimide) or 5-(4-aminophenyl)-10,15,20-tri(4-maleimidophenyl)zinc porphyrin, tris(tetrabutylammonium) salt (ZnP-maleimide) in CH_3CN at 30 °C for 2 h. The DNA–porphyrin conjugates were purified by a reversed-phase HPLC (same conditions as described above). MALDI-TOF-MS (negative mode): DNA–FbP: calcd 4035.7 [M−H]; obsd **1-FbP**: 4036.5; **2-FbP**: 4035.9; **3-FbP**: 4037.7; **4-FbP**: 4036.7. DNA–ZnP: calcd 4097.6 [M−H]; obsd **1-ZnP**: 4098.2; **2-ZnP**: 4097.2; **3-ZnP**: 4098.3; **4-ZnP**: 4099.3.

4.4. UV–vis and fluorescence spectroscopy

The UV–vis and fluorescence spectra were obtained in solutions containing 2.0 μM DNA, 10 mM phosphate (pH 7.0), and 1.0 M NaCl. All the samples were gradually annealed from 85 °C to 10 °C. Melting profiles were obtained by increasing the temperature from 10 °C to 75 °C at a ratio of 1.0 °C/min using the absorbance change at 260 nm with the same sample above. The melting temperatures (°C) are as follows: **1-FbP**, 56.4 °C; **2-FbP**, 54.0 °C; **3-FbP**, 52.5 °C; **4-FbP**, 48.8 °C; **1-ZnP**, 55.4 °C; **2-ZnP**, 53.4 °C; **3-ZnP**, 44.6 °C; **4-ZnP**, 32.2 °C.

4.5. Circular dichroism (CD) spectroscopy

CD spectra were acquired on a JASCO J-710 spectropolarimeter. Measurements were carried out at 20 °C in a solution containing 10 μM DNA–porphyrin conjugate, 10 mM phosphate buffer (pH 7.0), and 1.0 M NaCl.

4.6. Fluorescence lifetime measurements

Fluorescence decays were acquired by the single photon counting method using a streak scope (Hamamatsu Photonics, C4334-01). Samples were excited with a second harmonic generation (420 nm) of a Ti-:Sapphire laser (Spectra Physics, Tsunami 3941-M1BB, fwhm 100 fs). Measurements were carried out at 23 °C in a solution containing 2.0 μM DNA–porphyrin conjugate, 10 mM phosphate buffer (pH 7.0), and 1.0 M NaCl. Photos in 590–620 nm for DNA–ZnP and in 700–740 nm for DNA–FbP were collected for the calculation of fluorescence lifetimes.

Acknowledgements

This work has been partly supported by a Grant-in-Aid for Scientific Research (Project 17105005 and others) from the Ministry of Education, Culture, Sports, Science and Technology (MEXT) of Japanese Government.

References and notes

1. Hoeben, F. J.; Jonkheijm, P.; Meijer, E. W.; Schenning, A. P. H. J. *Chem. Rev.* **2005**, *105*, 1491–1546.
2. Schenning, A. P. H. J.; Meijer, E. W. *Chem. Commun.* **2005**, 3245–3258.
3. Hill, D. J.; Mio, M. J.; Prince, R. B.; Hughes, T. S.; Moore, J. S. *Chem. Rev.* **2001**, *101*, 3893–4012.
4. Kobuke, Y.; Ogawa, K. *Bull. Chem. Soc. Jpn.* **2003**, *76*, 689–708.
5. Choi, M.; Yamazaki, T.; Yamazaki, I.; Aida, T. *Angew. Chem., Int. Ed.* **2004**, *43*, 150–158.
6. Maiti, N. C.; Mazumdar, S.; Periasamy, N. *J. Phys. Chem. B* **1998**, *102*, 1528–1538.
7. Kano, K.; Fukuda, K.; Wakami, H.; Nishiyabu, R.; Pasternack, R. F. *J. Am. Chem. Soc.* **2000**, *122*, 7494–7502.
8. Schwab, A. D.; Smith, D. E.; Rich, C. S.; Young, E. R.; Smith, W. F.; de Paula, J. C. *J. Phys. Chem. B* **2003**, *107*, 11339–11345.
9. Okada, S.; Segawa, H. *J. Am. Chem. Soc.* **2003**, *125*, 2792–2796.
10. Schwab, A. D.; Smith, D. E.; Bond-Watts, B.; Johnston, D. E.; Hone, J.; Johnson, A. T.; de Paula, J. C.; Smith, W. F. *Nano Lett.* **2004**, *4*, 1261–1265.
11. Nakamura, M.; Ohtoshi, Y.; Yamana, K. *Chem. Commun.* **2005**, 5163–5165.
12. Mayer-Enthart, E.; Wagenknecht, H. A. *Angew. Chem., Int. Ed.* **2006**, *45*, 3372–3375.
13. Ferentz, A. E.; Keating, T. A.; Verdine, G. L. *J. Am. Chem. Soc.* **1993**, *115*, 9006–9011.
14. Kruper, W. J., Jr.; Chamberlin, T. A.; Kochanny, M. *J. Org. Chem.* **1989**, *54*, 2753–2756.
15. Base pair models were produced from the central two base pairs of the cystal structures of d(CGCGA*AT*TCGCG)$_2$ (PDB, 1DOU) and d(CGCGT*TA*ACGCG)$_2$ (PDB, 194D) for AT/AT and TA/TA base pairs, respectively.
16. Balaz, M.; Holmes, A. E.; Benedetti, M.; Rodriguez, P. C.; Berova, N.; Nakanishi, K.; Proni, G. *J. Am. Chem. Soc.* **2005**, *127*, 4172–4173.
17. Balaz, M.; Li, B. C.; Jockusch, S.; Ellestad, G. A.; Berova, N. *Angew. Chem., Int. Ed.* **2006**, *45*, 3530–3533.
18. Pasternack, R. F.; Francesconi, L.; Raff, D.; Spiro, E. *Inorg. Chem.* **1973**, *12*, 2606–2611.
19. Hoard, J. L. *Science* **1971**, *174*, 1295–1302.
20. Berova, N.; Nakanishi, K. *Circular Dichroism, Principles and Applications*; Berova, N., Nakanishi, K., Woody, R. W., Eds.; Wiley-VCH: New York, NY, 2000; pp 337–382.
21. Johnson, W. C. *Circular Dichroism, Principles and Applications*; Berova, N., Nakanishi, K., Woody, R. W., Eds.; Wiley-VCH: New York, NY, 2000; pp 703–718.
22. Allemann, R. K.; Egli, M. *Chem. Biol.* **1997**, *4*, 643–650.